Anisotropic index of refraction and structural properties of hexagonal boron nitride epilayers probed by spectroscopic ellipsometry

M. A. McKay, J. Li, J. Y. Lin, and H. X. Jiang[a]

AFFILIATIONS

Department of Electrical and Computer Engineering, Texas Tech University, Lubbock, Texas 79409, USA

[a]**Author to whom correspondence should be addressed:** hx.jiang@ttu.edu

ABSTRACT

The anisotropic index of refraction of $200\,\mu$m thick boron-10 enriched hexagonal boron nitride (h-BN) freestanding epilayers grown by metalorganic chemical vapor deposition has been measured using spectroscopic ellipsometry in the UV (4.0–5.1 eV) spectral range. It was found that the index of refraction for the polarization mode with an electric field perpendicular to the c-axis (ordinary, n_o) is much higher than that with an electric field parallel to the c-axis (extraordinary, n_e). By inclusion of turbostratic- (t-) phase layers within h-BN having an average inclination angle (θ) with respect to the ideal c-plane, a simple method for quantifying θ has been deduced. Our results revealed that the presence of t-phase layers decreases the optical anisotropy of h-BN and that a signature of improved crystalline quality is an increase in the ordinary index of refraction (n_o) as a result of the average incline angle θ approaching 0° and predicted that $n_o = 2.7$ and $n_e = 1.5$ at 280 nm for single crystalline h-BN epilayers. More importantly, our results demonstrated that spectroscopic ellipsometry is an effective technique for characterizing the crystalline quality of h-BN epilayers with the advantages of being noninvasive and highly sensitive.

Published under license by AIP Publishing. https://doi.org/10.1063/1.5134908

I. INTRODUCTION

Hexagonal boron nitride (h-BN) has gained increasing attention in recent years, due to its unique physical properties and potential applications. Properties such as wide bandgap (>6 eV),[1–8] high temperature and chemical stability,[9] large optical absorption near the band edge,[10–12] and large thermal neutron capture cross section of isotope B-10,[13,14] make h-BN a promising material for applications in high efficiency deep ultraviolet (DUV) optoelectronics,[1–8,15–19] solid-state neutron detectors,[20–24] and single photon emitters.[25–27] Due to the layered structure of h-BN and its similar lattice constant to graphene (~1.6% mismatch of in-plane lattice constants), h-BN is also considered as an ideal substrate and dielectric separation or gate layer for graphene and other van der Waals stacked heterostructures.[28–31] Most notably, detectors fabricated from thick B-10 enriched h-BN epilayers have demonstrated the highest detection efficiency for thermal neutrons among solid-state detectors to date (at 58% for 1 mm^2 detectors and 50% for 30 mm^2 detectors).[23]

Despite the growing number of studies on h-BN, the material is still in its early development stage. While bulk h-BN materials synthesized by high temperature/pressure techniques[1] or via precipitation from molten metal solvents (or metal flux technique) at atmospheric pressure[2] and hence mono- or few-layer h-BN exfoliated from these small bulk crystals generally exhibit high crystalline quality, only small crystals with sizes up to a few millimeters have been produced so far and there are significant difficulties in scalability. On the other hand, it was shown that the overall detection efficiency of neutron detectors fabricated from thick h-BN epilayers is still limited by the charge collection efficiency, which is directly correlated with the overall material quality.[23] The ability for synthesizing wafer-scale h-BN epilayers with high crystalline quality and large thickness is necessary for technologically significant applications such as neutron detectors. This, however, requires effective material characterization techniques to provide insights, which will enable viable approaches to synthesizing h-BN epilayers with improved material quality.

Due to the strong bond between B-N and high melting temperature of h-BN, it is difficult to crystallize BN epilayers into the single crystalline hexagonal phase. As such, h-BN epilayers

synthesized by thin film growth techniques such as chemical vapor deposition (CVD) and metalorganic chemical vapor deposition (MOCVD) typically contain turbostratic- (t-) phase layers. Turbostratic is a term used to describe a crystal structure in which the basal plane (in this case the c-plane) has slipped out of alignment. It is apparent that the presence of t-phase in an h-BN wafer will reduce its overall crystalline quality and hence the performance of its associated devices. To further advance the development and applications of h-BN, it is important to gain a more complete understanding of optical and structural properties of wafer-scale thick h-BN epilayers, from which practical devices such as neutron detectors can be constructed.

One of the methods to assess the crystalline quality of h-BN is to quantify the amount of inclusions of t-phase regions within the h-phase BN. It has been noticed that the microscopic c-planes of the h-BN layers exhibit an average inclination angle (θ) from the ideal c-plane.[32–34] This average inclination angle (θ) in a 3 nm thick h-BN has been previously probed by the near-edge x-ray
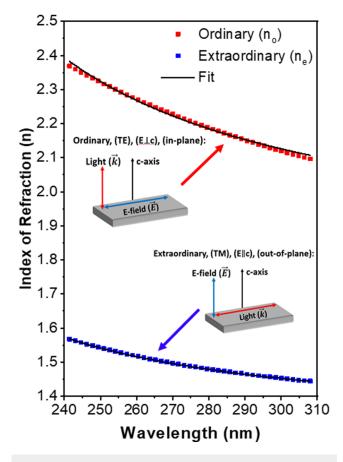

FIG. 1. Indices of refraction of a 200 μm thick B-10 enriched h-BN epilayer in the UV range measured using spectroscopic ellipsometry for both polarization modes with electric field perpendicular (n_o) and parallel (n_e) to the c-axis as functions of incident wavelength λ. The inset is a depiction of the ordinary (n_o) and extraordinary (n_e) polarization modes.

absorption fine structure (NEXAFS) technique.[32] However, NEXAFS is an elaborate technique and cannot be routinely utilized to characterize h-BN materials. It is anticipated that the optical constants or index of refraction are highly anisotropic for light polarization along the c-axis (ordinary, n_o, $E \perp$ c-axis) or along the c-plane (extraordinary, n_e, $E \parallel$ c-axis) in h-BN due to its layered structure.[33–38] Such an effect is depicted in the insets of Fig. 1. The index of refraction of h-BN depends on its layered microstructure or deviation of its crystal structure from the single crystalline hexagonal phase, such as the inclusion of t-phase layers as well as the average orientations of the h-BN layers. Layers within h-BN that are not completely parallel to the ideal c-plane will decrease the anisotropy of the optical constants. Therefore, characterizing the anisotropy of optical constants presents an effective method for probing the crystalline quality of h-BN.

We report here the successful growth and characterization of indices of refraction of a thick B-10 enriched h-BN epilayer ($\sim$200 μm in thickness) in both the ordinary (n_o) and extraordinary (n_e) polarization modes via spectroscopic ellipsometry (SE). Expanding on the microstructure model of Schubert et al.,[34] we describe here a method for determining the average orientation of h-BN layers relative to the ideal c-plane, which can be used to calibrate the h-BN crystalline quality, as well as to predict the change in the index of refraction of h-BN due to the presence of various inclinations of t-phase layers and the average orientations of layers. We believe that the method of characterization developed here provides a simple and effective new venue for monitoring the crystalline quality to support further development of the epitaxial growth technology and device applications of h-BN epilayers.

II. EXPERIMENTS

B-10 enriched (99.9%) h-BN epilayers of about 200 μm in thickness were grown by metalorganic chemical vapor deposition (MOCVD) on c-plane sapphire substrates of 4 in. in diameter. Trimethylboron (TMB) and ammonia (NH$_3$) were used as precursors for B and N, respectively, and nitrogen was used as a carrier gas. The epigrowth temperature was about 1500 °C.[39] Due to the sizeable difference in thermal expansion coefficients between h-BN and sapphire substrate, h-BN epilayer tends to mechanically self-separate from the substrate during the cooling process, producing a 200 μm thick freestanding h-BN wafer and the detailed information about growth and basic properties of h-BN can be found in our previous publications.[22,23,39]

Spectroscopic ellipsometry is a noninvasive optical technique for investigating the dielectric properties of materials.[33,34] Initially, generalized Mueller matrix ellipsometry was performed on the sample at 0°, 45°, and 90° of rotation with respect to the measurement stage to confirm that it is a c-plane sample and that there is a negligible effective in-plane anisotropy. We focus here on analyzing spectroscopic ellipsometry data to determine the indices of refraction and microstructure of h-BN. Measurements were performed using spectroscopic ellipsometry (SE) (M-2000XI Ellipsometer by J. A. Woollam Company) in the spectral range of 4.0–5.1 eV at five angles of incidence (Φ = 45–75). These angles of incidence were chosen to measure at angles below, near, and above the Brewster angle of h-BN. The results were fit with a two-layer model

(CompleteEASE by J. A. Woollam Company) that included a 17 nm Cauchy layer on the top of the freestanding h-BN epilayer to account for the presence of a thin amorphous BN buffer layer deposited prior to the growth of h-BN epilayer as well as possible oxidation in air. The bottom epilayer model consisted of a uniaxial anisotropic Cauchy fit to extract both the ordinary and extraordinary index of refraction from the raw spectroscopic ellipsometry data.

III. RESULTS AND DISCUSSIONS

The results for the ordinary (n_o, $\vec{E} \perp$ c-axis) and extraordinary (n_e, $\vec{E} \parallel$ c-axis) index of refraction are shown in Fig. 1. Note that h-BN displays a sizeable negative birefringence ($\Delta n = n_e - n_o \approx -0.8$) due to its layered structure, which is significantly higher than the birefringence found in, for instance, quartz (SiO$_2$, $\Delta n = +0.011$),[40] an example of a birefringent crystal that is widely used in laser devices and other optoelectronic devices. The huge optical anisotropy in the UV range arises from the excitonic effects in h-BN. Such a vast rise in n_o arises from the excitonic effects in h-BN.[3–7,41,42] The two-dimensional layered structure of h-BN crystal produces a large charge density inhomogeneity along the c-axis and thus causing the excitons to be tightly confined within the layers. For the electric field polarization perpendicular to the c-axis (n_o), parity selection rules allow excitons from interband transitions of the same parity with respect to the mirror plane within each layer, and consequently, they exhibit large oscillator strength.[3–6,41,42] Therefore, they contribute to n_o but not to n_e, and thus the birefringence of h-BN shows a significant increase in the UV spectral range.

It was shown that the electronic response of a material can be described through the single-oscillator approximation when the photon energy is much smaller than the lowest energy gap of the material.[35] Because the energy gap of h-BN is above 6 eV,[1–8] the measured indices of refraction covering the incident wavelength between 241 and 310 nm for both ordinary and extraordinary polarization modes were then fitted using a single-oscillator model, which shows that the dispersive index of refraction as a function of incident wavelength, λ, can be described as follows:

$$n(\lambda) = \sqrt{1 + \frac{A\lambda^2}{\lambda^2 - \lambda_0^2}}, \qquad (1)$$

where the parameters λ_0 and A are related to the energy bandgap and the electric-dipole oscillator strength associated with

transitions at incident wavelengths, λ, respectively.[35,43] As shown in Fig. 1, the equation fits very well to the data, and the fitted values were $\lambda_{0o} = 167.7$ nm, $\lambda_{0e} = 165.9$ nm, $A_o = 2.42$, and $A_e = 0.77$, respectively. Note that the bandgap related parameter λ_0 is almost identical for both the ordinary (n_o) and extraordinary (n_e) polarization modes. Once the index of refraction dispersion is established, we assume that the electronic contribution to the index of refraction for both ordinary and extraordinary polarization modes obeys a simple Phillips-van Vechten model.[44,45] This model assumes that all valence-to-conduction band transitions that contribute to the material's electronic dielectric function can be described by a single transition at an average frequency, which is known as the Penn gap.[46] Under this assumption, the index of refraction as a function of incident wavenumber, σ, is given by
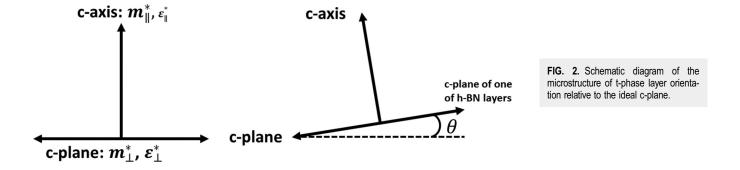
$$n(\sigma) = \sqrt{1 + \frac{\sigma_{P0}^2}{\sigma_0^2 - \sigma^2}}, \qquad (2)$$

where σ_0 and σ_{P0} are, respectively, the Penn gap and average plasma frequency of valence electrons involved in allowed transitions. From Eqs. (1) and (2), we relate the electric-dipole oscillator strength to the plasma frequency,

$$\sigma_{P0}^2 = \frac{Ac^2}{\lambda_0^2} = \frac{4\pi Nq^2}{m^* \varepsilon_r \varepsilon_0}, \qquad (3)$$

where c is the velocity of light in vacuum, N is the charge carrier concentration, q is the elementary charge, m^* is the electron effective mass, ε_r is the dielectric constant of h-BN, and ε_0 is the vacuum permittivity.

The strong bond between B-N makes high growth temperatures a necessary condition for attaining h-BN films with high crystalline quality. As such, for most h-BN thin films grown today or earlier, the crystal structure still deviates from the pure single crystalline hexagonal structure. It was shown that one of the effective methods to assess the crystalline quality of h-BN is to quantify the amount of inclusions of t-phase regions within the h-phase BN,[32] by interpreting the microscopic c-planes of the h-BN layers exhibiting an average inclination angle (θ) from the ideal c-plane,[32–34] as illustrated in Fig. 2. In the context of Fig. 2, single crystalline h-BN epilayers should have a value of $\theta = 0$. Figure 3 schematically

FIG. 2. Schematic diagram of the microstructure of t-phase layer orientation relative to the ideal c-plane.

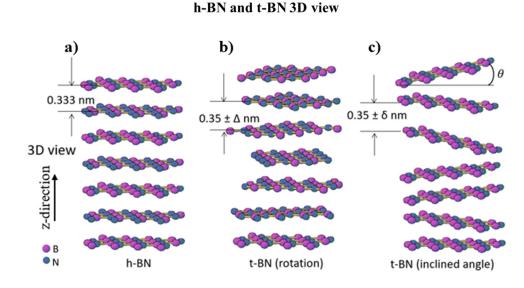## h-BN and t-BN 3D view

FIG. 3. Depiction of h-BN compared to two different types of turbostratic (t-phase) BN: (a) h-BN with periodicity in all three dimensions; (b) t-phase layers have rotated around the c-axis (little to no periodicity in the z-direction); (c) t-phase layers with an average incline angle θ relative to the ideal c-plane. Both (b) and (c) produce an increase in the distribution of the distance between neighboring layers.

illustrates possible structural configurations of h-BN and that h-BN epilayers grown by CVD[32] and MOCVD[16–18,22–24,39,47,48] or even h-BN bulk crystals grown by the metal flux technique[49] unavoidably contain t-phase components, especially when the growth conditions are not optimized. The observation of an average incline angle θ is a signature of the presence of t-phase component in addition to an enlarged distance between two adjacent layers over that in a pure single crystalline h-BN. In Fig. 3, t-phase could mean individual layers have rotated around the ideal c-axis (changing the crystallographic direction), as schematically showed in Fig. 3(b). Moreover, t-phase could also mean that individual layers are tilted with respect to the c-plane, or a combination of both, a case which is depicted in Fig. 3(c). The combination of both tilt and rotation averaged over all the layers maps the c-axes into a cone shape in 3D space.[33,34] The t-phase layers will automatically increase the distribution of the distance between the adjacent layers. The enlarged structural imperfection not only decreases the optical anisotropy (as it disrupts the layered structure), but also enlarges the average incline angle θ.

Thin h-BN layers with a thickness of ~3 nm have been recently probed by transmission electron microscopy (TEM) and it was found that the diffraction patterns of h-BN samples consisted of two rings, corresponding to two predominant crystallographic domains coexisting in the sample with an angle of rotation with respect to the ideal c-axis [Fig. 3(c)] between them of ~11.1°.[44] The same materials were further examined using NEXAFS method, and the results showed that each layer of h-BN could have an average inclined angle with respect to the ideal c-plane, as illustrated in Figs. 2 and 3(b), and this angle is random from layer to layer with a measured average value of 15.83° for postannealed h-BN epilayers and 22.17° for as-grown h-BN.[32] Another study showed that a wide range of angles can be forced onto the material's crystalline structure by applying a bias voltage to the substrate during growth and concluded that this average incline angle affects the optical anisotropy as well as the values of index of refraction for both ordinary and extraordinary polarization modes.[33] These prior studies

suggested that monitoring the optical anisotropy can provide useful insights into the average inclination angle (θ), which correlates directly with the crystalline quality.

For spectroscopic ellipsometry measurements with fixed orientations of light propagation and electric field, the effective mass and dielectric constant will be affected by the orientation of the c-axes as illustrated in Fig. 2, according to the equations,

$$m_{\perp}^{*} = \sqrt{m_{\perp}^{2}\cos^{2}\theta + m_{\parallel}^{2}\sin^{2}\theta}, \tag{4a}$$

$$\varepsilon_{\perp}^{*} = 0.25 \left[(3 + \cos 2\theta)\, \varepsilon_{\perp} + (1 - \cos 2\theta)\, \varepsilon_{\parallel} \right], \tag{4b}$$

$$m_{\parallel}^{*} = \sqrt{m_{\perp}^{2}\sin^{2}\theta + m_{\parallel}^{2}\cos^{2}\theta}, \tag{4c}$$

$$\varepsilon_{\parallel}^{*} = (n_{\parallel}\cos\theta)^{2} + (n_{\perp}\sin\theta)^{2}. \tag{4d}$$

Equations (4a) and (4c) were derived using Fig. 2, by projecting θ onto assumed parallel and perpendicular effective masses. Equations (4b) and (4d) are from the work of Schubert et al.[34] From Eqs. (3) and (4), by noting a constant charge carrier concentration for n_o and n_e of the same sample, and $\lambda_{0o} = \lambda_{0e}$, we obtain the following equation, which can be used to find the average orientation of the h-BN layers relative to the ideal c-plane, θ,

$$\frac{A_{\perp}}{A_{\parallel}} = \left[\frac{\left(\dfrac{m_{\perp}}{m_{\parallel}}\right)^{2}\tan^{2}\theta + 1}{\left(\dfrac{m_{\perp}}{m_{\parallel}}\right)^{2} + \tan^{2}\theta} \right]^{1/2}$$

$$* \left[\frac{\varepsilon_{\perp}\sin^{2}\theta + \varepsilon_{\parallel}\cos^{2}\theta}{0.25\left[(3 + \cos 2\theta)\,\varepsilon_{\perp} + (1 - \cos 2\theta)\,\varepsilon_{\parallel}\right]} \right]. \tag{5}$$

By using the measured A_o and A_e values from Fig. 1, we obtain an average θ for the 200 μm thick sample used in this study. This average tilt angle quantifies how much, on average, of the h-BN layers are aligned parallel to the ideal c-plane. From just the measured indices of refraction, Eqs. (1) and (5), we can determine the average incline angle of t-phase layers within an h-BN sample.

Because there are scattered data among published values for the effective masses and dielectric constants of h-BN,[50–53] in Fig. 4, we plot the ratio of A_o /A_e as a function of θ from Eqs. (4) and (5). The differences in the effective masses and dielectric constants for different polarization modes lead to the optical anisotropy of h-BN. We have chosen the values $m_\perp^* = 0.26 \, m_o$ (M → Γ), $m_\parallel^* = 2.21 \, m_o$ (M → L),[50] $\varepsilon_\perp = 4.98$, and $\varepsilon_\parallel = 3.03$[52] for the rest of the analysis. Using these values, we obtain an average θ, varying from 6.47° to

11.93°, with an average incline angle of $\theta \approx 9°$ for the sample used in this study, as shown in the inset (a) of Fig. 4. Note that any combination of effective mass and dielectric constants does not alter the derived value of θ significantly. This average inclined angle of $\theta \approx 9°$ is significantly smaller than those of previously published values of a 3 nm thick postannealed and as-grown h-BN layers exhibiting average θ of 15.83° and 22.17°, respectively,[32] signifying a better crystalline quality of the sample grown by used in the present study. Based on the observation of reduced value of θ for the sample studied here compared to CVD grown films,[32] we believe that our MOCVD grown thick h-BN epilayers have a better crystalline quality than those grown by CVD methods.[32]

We can conclude that the sample consists of a variety of crystallographic domains, meaning individual layers within the sample may have t-phase inclusion within h-BN layers, and the layers containing t-phase have a random average incline angle θ relative to the ideal c-plane. The measured value of $\theta = 9°$ is an average incline angle of all the layers within the sample relative to the ideal c-plane. This understanding is also consistent with the x-ray diffraction (XRD) θ-2θ scan result of a typical h-BN epilayer deposited on sapphire, as shown in the inset (b) of Fig. 4. While the h-phase layers produce a sharp (0002) peak around 26.7°, t-phase layers produce a shoulder at a smaller angle of about 26°,[12,47,48] consistent with an expected increase in the distance between the adjacent layers in the t-phase. The t-phase XRD peak is also broader than the h-phase peak as a result of a random distribution of the distance between two adjacent layers, around an average distance of 3.5 Å as schematically illustrated in Figs. 3(b) and 3(c).

The use of the measured value of $\theta = 9°$ as well as Eqs. (4) and (5) allows us to predict what the index of refraction for both ordinary and extraordinary polarization modes would look like in h-BN epilayers having a single crystalline hexagonal phase, or equivalent for the case of $\theta = 0°$. Assuming that the free carrier concentration remains unchanged, we plot in Fig. 5 the calculated ordinary and extraordinary refraction indices as functions of wavelength for h-BN in a single crystalline h-phase (or $\theta = 0$) together with those of measured values for the sample used in the present study. As the average incline angle θ decreases, the optical anisotropy increases; thus, the ordinary and extraordinary indices of refraction get further apart. It appears, however, that the extraordinary index of refraction (n_e) does not decrease significantly. The negligible change in the extraordinary index of refraction as θ approaches zero is due to the excitonic effects taking place in h-BN.[3–7,42] A signature of improved crystalline quality is an increase in the ordinary index of refraction (n_o) as a result of the average incline angle θ approaching 0°. Figure 5 makes it apparent that the variation in prior published values for the optical constants of h-BN, specifically in the indices of refraction,[35–38] is a consequence of different h-BN samples containing varying fractions of t-phase layers with different average inclined angles, because numerous types of materials such as small bulk crystals, thin films, or powders, as well as materials synthesized by the same method but prepared at different growth conditions were used. The fraction of t-phase layers within h-BN samples can vary widely depending on the growth method, growth conditions, and thickness of the sample. For example, the fraction of t-phase layers within h-BN epilayers can vary significantly among samples grown by MOCVD
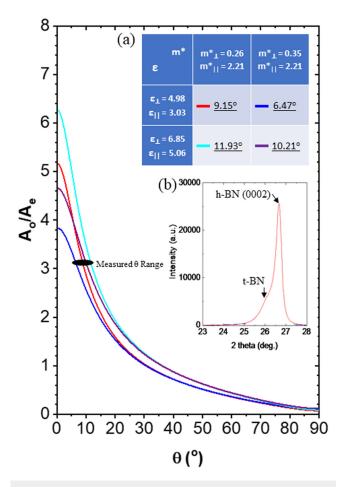

FIG. 4. Variation of the birefringence (A_o /A_e) as a function of the average c-axis orientations, θ, for different values of effective masses and dielectric constants, using Eqs. (1) and (5). Inset (a) is a table containing different values of effective masses and dielectric constants used in obtaining the plots. The thick black line between 6° and 12° is the value of A_o /A_e = 3.14. The color of the curve corresponds to the color of the resultant angle θ in the inset (a). Inset (b) is an XRD θ–2θ scan of a representative h-BN epilayer grown by MOCVD.
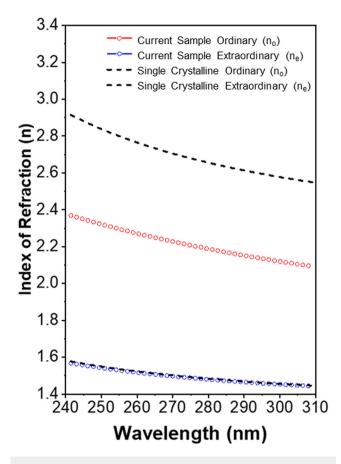
FIG. 5. Measured index of refraction of the h-BN sample used in the present study (open circles, $\theta \approx 9°$) and expected index of refraction of a pure h-phase single crystal h-BN (dotted lines, $\theta = 0°$) in the UV range for both ordinary (n_o) and extraordinary (n_e) polarizations as a function of incident photon wavelength λ.

under different growth conditions, which will result in different values in the average inclined angle θ. Our results thus suggest that the presence of t-phase layers should be considered when analyzing the optical constant and XRD measurement data of h-BN. Furthermore, our results revealed that measuring the average inclined angle θ [using just Eqs. (1) and (5)] or optical constant anisotropy via spectroscopic ellipsometry provides an effective method for monitoring the crystalline quality of h-BN epilayers produced under different growth conditions and thereby offers valuable insights for further improving the epitaxial growth processes.

IV. CONCLUSION

Ordinary ($\vec{E} \perp$c-axis) and extraordinary ($\vec{E} \parallel$ c-axis) anisotropic indices of refraction of a thick h-BN epilayer produced by MOCVD have been measured over a spectral range slightly below the bandgap (4.0–5.1 eV). The results have demonstrated that the index of refraction is anisotropic and uniaxially negative, with the ordinary (n_o) indices of refraction being higher than the

extraordinary (n_e) indices of refraction and predicted that $n_o = 2.7$ and $n_e = 1.5$ at 280 nm for samples crystallized into a single crystalline hexagonal phase. The measured index of refraction of h-BN can vary in a wide range due to the presence of t-phase layers within h-BN, which possess microscopic c-axes exhibiting an average inclination angle (θ) from the plane of the h-BN films. This average inclination angle (θ) was determined via a single-oscillator model and a Phillips-van Vechten model. This technique also allowed us to predict what the indices of refraction are for both ordinary and extraordinary at various orientations of average c-axes. It will be useful in the future work to include establishing a relationship between XRD, TEM, and ellipsometry results to examine the distribution of t-phase layers (or the distribution of angle θ) within the more ideal h-BN. The presence of inhomogeneity exacerbates the average incline angle θ, which decreases the effect of optical anisotropy, including the indices of refraction, dielectric function, and optical absorption. By just using Eqs. (1) and (5) established in this work, we can reliably determine the average incline angle of t-phase layers within an h-BN sample, and potentially other 2D stacked materials. We believe that the anisotropy in indices of refraction for ordinary and extraordinary polarization modes and the technique of determining the average c-axes orientations established in this work provide an effective venue to guide the further development of growth processes and characterization of h-BN as well as of other 2D optoelectronic semiconductors in the quest of attaining high crystalline quality materials.

REFERENCES

[1]K. Watanabe, T. Taniguchi, and H. Kanda, Nat. Mater. **3**, 404 (2004).
[2]Y. Kubota, K. Watanabe, O. Tsuda, and T. Taniguchi, Science **317**, 932 (2007).
[3]B. Arnaud, S. Lebègue, P. Rabiller, and M. Alouani, Phys. Rev. Lett. **96**, 026402 (2006).
[4]B. Arnaud, S. Lebègue, P. Rabiller, and M. Alouani, Phys. Rev. Lett. **100**, 189702 (2008).
[5]L. Wirtz, A. Marini, M. Grüning, C. Attaccalite, G. Kresse, and A. Rubio, Phys. Rev. Lett. **100**, 189701 (2008).
[6]L. Wirtz, A. Marini, and A. Rubio, Phys. Rev. Lett. **96**, 126104 (2006).
[7]X. K. Cao, B. Clubine, J. H. Edgar, J. Y. Lin, and H. X. Jiang, Appl. Phys. Lett. **103**, 191106 (2013).
[8]T. C. Doan, J. Li, J. Y. Lin, and H. X. Jiang, Appl. Phys. Lett. **109**, 122101 (2016).
[9]O. Gafri, A. Grill, D. Itzhak, A. Inspektor, and R. Avni, Thin Solid Films **72**, 523 (1980).
[10]T. Sugino, K. Tanioka, S. Kawasaki, and J. Shirafuji, Jpn. J. Appl. Phys. **36**, L463 (1997).
[11]A. Zunger, A. Katzir, and A. Halperin, Phys. Rev. B **13**, 5560 (1976).
[12]J. Li, S. Majety, R. Dahal, W. P. Zhao, J. Y. Lin, and H. X. Jiang, Appl. Phys. Lett. **101**, 171112 (2012).
[13]G. F. Knoll, *Radiation Detection and Measurement*, 4th ed. (John Wiley & Sons, 2010).
[14]O. Osberghaus, Z. Phys. **128**, 366 (1950).
[15]K. Watanabe and T. Taniguchi, Phys. Rev. B **79**, 193104 (2009).

[16] R. Dahal, J. Li, S. Majety, B. N. Pantha, X. K. Cao, J. Y. Lin, and H. X. Jiang, Appl. Phys. Lett. **98**, 211110 (2011).

[17] S. Majety, J. Li, X. K. Cao, R. Dahal, B. N. Pantha, J. Y. Lin, and H. X. Jiang, Appl. Phys. Lett. **100**, 061121 (2012).

[18] H. X. Jiang and J. Y. Lin, ECS J. Solid State Sci. Technol. **6**, Q3012 (2017).

[19] D. A. Laleyan, S. Zhao, S. Y. Woo, H. N. Tran, H. B. Le, T. Szkopek, H. Guo, G. A. Botton, and Z. Mi, Nano Lett. **17**, 3738 (2017).

[20] J. Uher, S. Pospisil, V. Linhart, and M. Schieber, Appl. Phys. Lett. **90**, 124101 (2007).

[21] F. P. Doty, U.S. patent 6,727,504 (27 April 2004).

[22] A. Maity, T. C. Doan, J. Li, J. Y. Lin, and H. X. Jiang, Appl. Phys. Lett. **109**, 072101 (2016).

[23] A. Maity, S. J. Grenadier, J. Li, J. Y. Lin, and H. X. Jiang, J. Appl. Phys. **123**, 044501 (2018); J. Appl. Phys. **125**, 104501 (2019); Appl. Phys. Lett. **114**, 222102 (2019).

[24] K. Ahmed, R. Dahal, A. Weltz, J. J.-Q. Lu, Y. Danon, and I. B. Bhat, Appl. Phys. Lett. **110**, 023503 (2017).

[25] R. Bourrellier, S. Meuret, A. Tararan, O. Stéphan, M. Kociak, L. H. G. Tizei, and A. Zobelli, Nano Lett. **16**, 4317 (2016).

[26] T. Q. P. Vuong, G. Cassabois, P. Valvin, A. Ouerghi, Y. Chassagneux, C. Voisin, and B. Gil, Phys. Rev. Lett. **117**, 097402 (2016).

[27] T. Tran, K. Bray, M. J. Ford, M. Toth, and I. Aharonovich, Nat. Nanotechnol. **11**, 37 (2016).

[28] A. K. Geim and I. V. Grigorieva, Nature **499**, 419 (2013).

[29] C. R. Dean, A. F. Young, I. Meric, C. Lee, L. Wang, S. Sorgenfrei, K. Watanabe, T. Taniguchi, P. Kim, K. L. Shepard, and J. Hone, Nat. Nanotechnol. **5**, 722 (2010).

[30] L. Britnell, R. V. Gorbachev, R. Jalil, B. D. Belle, F. Schedin, A. Mishchenko, T. Georgiou, M. I. Katsnelson, L. Eaves, S. V. Morozov, N. M. R. Peres, J. Leist, A. K. Geim, K. S. Novoselov, and L. A. Ponomarenko, Science **335**, 947 (2012).

[31] C. Dean, A. F. Young, L. Wang, I. Meric, G.-H. Lee, K. Watanabe, T. Taniguchi, K. Shepard, P. Kim, and J. Hone, Solid State Commun. **152**, 1275 (2012).

[32] S. H. Lee, H. Jeong, O. F. N. Okello, S. Xiao, S. Moon, D. Y. Kim, G. Y. Kim, J. I. Lo, Y. C. Peng, B. M. Cheng, H. Miyake, S. Y. Choi, and J. K. Kim, Sci. Rep. **9**, 10590 (2019).

[33] E. Franke, M. Schubert, H. Neumann, T. E. Tiwald, D. W. Thompson, J. A. Woollam, J. Hahn, and F. Richter, J. Appl. Phys. **82**, 2906 (1997).

[34] M. Schubert, B. Rheinländer, E. Franke, H. Neumann, J. Hahn, M. Röder, and F. Richter, Appl. Phys. Lett. **70**, 1819 (1997).

[35] S. Y. Lee, T. Y. Jeong, S. Jung, and K. J. Yee, Phys. Status Solidi B **256**, 1800417 (2018).

[36] S. L. Ren, A. M. Rao, and P. C. Eklund, Appl. Phys. Lett. **62**, 1760 (1993).

[37] D. C. Cameron, M. Z. Karim, and M. S. J. Hashmi, Thin Solid Films **236**, 96 (1993).

[38] T. H. Yuzuriha and D. W. Hess, Thin Solid Films **140**, 199 (1986).

[39] S. J. Grenadier, A. Maity, J. Li, J. Y. Lin, and H. X. Jiang, Appl. Phys. Lett. **112**, 162103 (2018).

[40] G. Ghosh, Opt. Comm. **163**, 95 (1999).

[41] D. M. Hoffman, G. L. Doll, and P. C. Eklund, Phys. Rev. B **30**, 6051 (1984).

[42] A. Segura, L. Artús, R. Cuscó, T. Taniguchi, G. Cassabois, and B. Gil, Phys. Rev. Mater. **2**, 024001 (2018).

[43] S. H. Wemple and M. DiDomenico, Jr., Phys. Rev. B. **3**, 1338 (1971).

[44] J. C. Phillips, Rev. Mod. Phys. **42**, 317 (1970).

[45] J. A. Van Vechten, Phys. Rev. **182**, 891 (1969).

[46] D. R. Penn, Phys. Rev. **128**, 2093 (1962).

[47] X. Yang, S. Nitta, K. Nagamatsu, S. Y. Bae, H. J. Lee, Y. Liu, M. Pristovsek, Y. Honda, and H. Amano, J. Cryst. Growth **482**, 1 (2018).

[48] T. C. Doan, J. Li, J. Y. Lin, and H. X. Jiang, AIP Adv. **4**, 107126 (2014).

[49] J. H. Edgar, T. B. Hoffman, B. Clubine, M. Currie, X. Z. Du, J. Y. Lin, and H. X. Jiang, J. Cryst. Growth **403**, 110 (2014).

[50] Y. N. Xu and W. Y. Ching, Phys. Rev. B **44**, 7787 (1991).

[51] F. Ferreira, A. Chaves, N. Peres, and R. Ribeiro, J. Opt. Soc. Am. B **36**, 674 (2019).

[52] A. Laturia, M. L. Van de Put, and W. G. Vandenberghe, npj 2D Mater. Appl. **2**, 6 (2018).

[53] R. Geick, C. H. Perry, and G. Rupprecht, Phys. Rev. **146**, 543 (1966).